THE JOURNAL OF PHYSICAL CHEMISTRY C

pubs.acs.org/JPCC Article

Pariser–Parr–Pople Model Based Configuration-Interaction Study of Linear Optical Absorption in Lower-Symmetry Polycyclic Aromatic Hydrocarbon Molecules

Pritam Bhattacharyya,* Deepak Kumar Rai,* and Alok Shukla*

Cite This: J. Phys. Chem. C 2020, 124, 14297–14305 Read Online

ACCESS | Metrics & More | Article Recommendations | Supporting Information

ABSTRACT: The electronic and optical properties of various polycyclic aromatic hydrocarbons (PAHs) with lower symmetry, namely, benzo[*ghi*]perylene ($C_{22}H_{12}$), benzo[*a*]coronene ($C_{28}H_{14}$), naphtho[2,3*a*]coronene ($C_{32}H_{16}$), anthra[2,3*a*]-coronene ($C_{36}H_{18}$), and naphtho[8,1,2-*abc*]coronene ($C_{30}H_{14}$), were investigated. We performed electron-correlated calculations using screened and standard parameters in the π-electron Pariser–Parr–Pople (PPP) Hamiltonian, and the correlation effects were included, both for ground and excited states, using multireference singles–doubles configuration-interaction (MRSDCI) methodology. The PPP model Hamiltonian includes long-range Coulomb interactions, which increase the accuracy of our calculations. The results of our calculations predict that, with the increasing sizes of the coronene derivatives, optical spectra are red-shifted, and the optical gaps decrease. In each spectrum, the first peak representing the optical gap is of moderate intensity, while the more intense peaks appear at higher energies. Our computed spectra are in good agreement with the available experimental data. For the purpose of comparison, we also performed first-principles time-dependent density-functional theory (TDDFT) calculations of the optical gaps of these molecules using Gaussian basis functions and found that they yielded values lower than our configuration-interaction (CI) results.

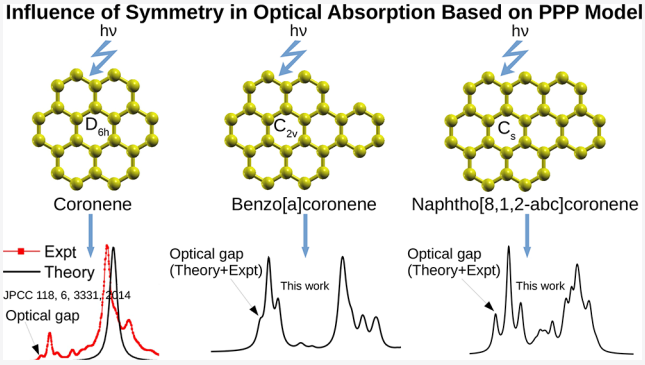

INTRODUCTION

Nowadays, π-conjugated molecules are used for manufacturing immensely effective as well as low-cost electronic devices such as organic thin-film (or field-effect) transistors (OTFTs or OFETs),[1−4] solar cells,[5,6] and light-emitting diodes (LEDs).[7−10] Polycyclic aromatic hydrocarbons (PAHs) are a class of π-conjugated molecules consisting of multiple aromatic rings, found to exist almost everywhere in the universe. A considerable percentage of carbon in the universe is present in the form of PAHs. From a technical point of view, this species of hydrocarbons is advantageous to society in several ways, but they are also carcinogenic to humans as well as other living beings. PAH molecules and their isomers exhibit unique properties and have high optical sensitivity. Therefore, to utilize this class of molecules in technological applications, a thorough investigation of their electronic structure and related properties is needed.

In an earlier work involving our group,[11] electronic structure and optical properties of coronene and related molecules with relatively high D_{6h} point group symmetry were studied. In this work, our aim is to study the lower symmetry (C_{2v} or lower) derivatives of coronene to understand the role which symmetry plays in determining the electronic and optical properties of PAHs. For this purpose, we employ a Pariser–Parr–Pople (PPP) model[12,13] based configuration-interaction (CI) methodology, established in several of our earlier works.[14−23] In particular, we study the optical properties of benzo[*ghi*]perylene ($C_{22}H_{12}$), benzo[*a*]coronene ($C_{28}H_{14}$), naphtho[2,3*a*]-coronene ($C_{32}H_{16}$), anthra[2,3*a*]coronene ($C_{36}H_{18}$), and naphtho[8,1,2-*abc*]coronene ($C_{30}H_{14}$). Several groups have studied these molecules experimentally. Khan measured the photoabsorption spectra of several cations of coronene and its derivatives, including benzo[*a*]coronene and naphtho[2,3*a*]-coronene.[24] Bagley et al. reported the optical absorption spectra of six- to nine-ring PAHs including benzo[*a*]coronene and naphtho[8,1,2-*abc*]coronene.[25] The ultraviolet spectra of many large PAHs, including benzo[*a*]coronene, were studied by Fetzer et al.[26] Fluorescence emission spectra of all the coronene derivatives, considered in this work, were experimentally studied by Acree et al.[27] Given the fact that no previous theoretical calculations of optical properties of these molecules exist, our

Received: February 27, 2020
Revised: May 16, 2020
Published: June 1, 2020

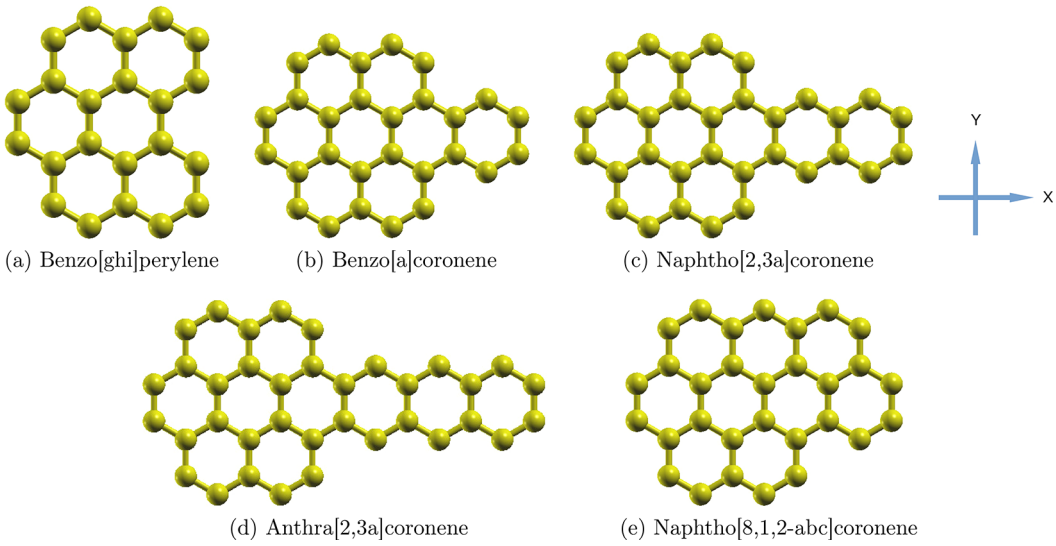

Figure 1. Schematic diagrams of coronene derivatives considered in this work. All the molecules are assumed to lie in the *xy*-plane. The yellow dots represent the carbon atoms, and the C−C bond lengths and bond angles are assumed to be 1.4 Å and 120°, respectively.

work is timely. These molecules are also interesting from another point of view: they can be seen as finite graphene fragments with hydrogen-passivated edges. The PAH molecules consist of aromatic rings of carbon atoms, in which the edge carbon atoms are passivated with the hydrogen atoms. One can imagine obtaining such molecules by cutting graphene sheets in those shapes, in a hydrogen-rich environment. Therefore, in the physics community, such molecules have been studied extensively under the name "finite graphene fragments" or graphene quantum dots.[21−23]

For the purpose of benchmarking, and comparing different computational approaches, we also performed first-principles time-dependent density functional theory (TDDFT) calculations of the optical gaps of these molecules using Gaussian basis functions. We find that the values of the optical gaps obtained from the TDDFT calculations are always lower than those obtained from our PPP model based CI calculations.

The remainder of this paper is organized as follows. In the next section, we discuss the theoretical methodology adopted in this work. We follow this by presenting and discussing our calculated optical absorption spectra for various molecules and compare our results to experiments, wherever possible. Finally, we present our conclusions.

THEORETICAL APPROACH AND COMPUTATIONAL DETAILS

Geometry. The molecules considered in this work are shown in Figure 1. It is assumed that all the molecules lie in the *xy*-plane, with uniform bond lengths and bond angles of 1.4 Å and 120°, respectively. All the molecules belong to the C_{2v} point group, along with a closed-shell $^1A_1$ electronic ground state, except naphtho[8,1,2-*abc*]coronene, which has a C_s point group and A' ground state. According to the dipole selection rule, the one-photon excited states have $^1A_1$ (*x*-polarized) and $^1B_2$ (*y*-polarized) symmetries for the C_{2v} molecules, while for the C_s molecule they have $^1A'$ (*xy*-polarized) symmetry. In this work, we only consider the excited states corresponding to photons polarized in the plane of the molecule.

Pariser−Parr−Pople (PPP) Model Hamiltonian. Calculations on the π-conjugated molecules considered in this paper were performed using a semiempirical approach, based upon the PPP model Hamiltonian,[12,13] which can be written as

$$H_{\mathrm{PPP}} = -\sum_{i,j,\sigma} t_{ij}(c_{i\sigma}^{\dagger}c_{j\sigma} + c_{j\sigma}^{\dagger}c_{i\sigma}) + U\sum_{i} n_{i\uparrow}n_{i\downarrow} + \sum_{i<j} V_{ij}(n_i - 1)(n_j - 1) \quad (1)$$

In the above equation, $c_{i\sigma}^{\dagger}$ ($c_{i\sigma}$) is the creation (annihilation) operator; i.e., it creates (annihilates) a π-electron with spin σ, localized on the i^{th} carbon atom. $n_{i\sigma} = c_{i\sigma}^{\dagger}c_{i\sigma}$ indicates the total number of π-electrons with spin σ, whereas $n_i = \sum_\sigma n_{i\sigma} = \sum_\sigma c_{i\sigma}^{\dagger}c_{i\sigma}$ denotes the total number of π-electrons on the i^{th} carbon atom. In the second and the third terms of eq 1, U and V_{ij} represent the on-site and long-range Coulomb interactions, respectively. t_{ij} denotes the one-electron hopping matrix element, which in this work has been restricted to nearest neighbors only, with the value t_0 = 2.4 eV, in agreement with our previous works on π-conjugated systems, such as conjugated polymers,[15,16] polycyclic aromatic hydrocarbons,[14,17−19] and graphene quantum dots.[20,21]

To parametrize the Coulomb interactions, we used the Ohno relationship[28]

$$V_{i,j} = U/\kappa_{i,j}(1 + 0.6117R_{i,j}^2)^{1/2} \quad (2)$$

where U denotes an on-site electron−electron repulsion term as discussed above; $\kappa_{i,j}$ indicates the dielectric constant of the system, using which we can include the screening effects; and $R_{i,j}$ is the distance between the i^{th} and j^{th} carbon atoms. In this paper, we computed the optical spectra using two types of Coulomb parameters: (a) screened parameters[29] [U = 8.0 eV, $\kappa_{i,j}$ = 2.0 ($i \neq j$) and $\kappa_{i,i}$ = 1.0] and (b) standard parameters[28] [U = 11.13 eV and $\kappa_{i,j}$ = 1.0]. We have observed that our earlier calculations performed using the screened parameters were in better agreement with the experimental results, as compared to the standard parameter-based ones.[16,17]

Optical Absorption Spectrum. For computing the optical absorption spectrum of an electronic system, we need to obtain a good representation of its ground- and excited-state wave functions. To that end, we performed the calculations using the multireference singles−doubles configuration-interaction

https://dx.doi.org/10.1021/acs.jpcc.0c01719
J. Phys. Chem. C 2020, 124, 14297−14305

(MRSDCI) methodology, as implemented in the computer program MELD.[30] For this purpose, first, we transformed the Hamiltonian from the site representation to the molecular orbital (MO) representation, which was achieved by performing mean-field restricted Hartree−Fock (RHF) calculations using a code based on the PPP model, developed in our group.[31] Then, a singles−doubles CI (SDCI) calculation was performed for both the ground state and excited states, by employing the transformed Hamiltonian and choosing a correct single reference wave function. The computed excited state wave functions were used to calculate the optical absorption spectrum at the SDCI level of theory. Next, the excited state wave functions contributing to the various peaks of optical spectra obtained using SDCI calculations were used as reference states for the MRSDCI calculations. Again the many-body wave functions of the excited states contributing to the various peaks of optical spectra, obtained using MRSDCI calculation, were analyzed and used as references for the next level of MRSDCI calculation with a lower cutoff of the contributing coefficients of the wave functions. This process is iterative and was continued until the computed optical spectra were converged with the previous one within an acceptable tolerance. In this study, we found the final cutoff value of 0.05 on the magnitude of contributing coefficients of the wave functions to be sufficient for achieving convergence. This implies that all the configurations whose coefficients in the MRSDCI wave function were more than 0.05 in magnitude were included in the list of reference configurations. This is a very stringent cutoff and fairly adequate for achieving convergence. In our group, the MRSDCI approach as described above has been used extensively to study a variety of molecules and clusters.[14−18,20,21,32−34]

For benzo[*ghi*]perylene, which is the smallest molecule considered in this study, we employed the quadruple configuration-interaction (QCI) approach to calculate the ground and the excited state wave functions as well as the optical absorption spectra. The QCI-level absorption spectra were compared to those computed using the MRSDCI approach, and very good agreement was obtained. Because QCI calculations are normally more accurate as compared to MRSDCI ones, the good agreement between the two sets of results validates the accuracy of the MRSDCI method. This is important because QCI calculations for the larger molecules are not computationally feasible, and therefore, only MRSDCI calculations were performed for them.

The wave functions of the ground and the excited states thus obtained are used to compute the electric dipole matrix elements, as well as the optical absorption spectra $\sigma(\omega)$, by employing the following formula

$$\sigma(\omega) = 4\pi\alpha \sum_i \frac{\omega_{i0}|\langle i|\hat{\mathbf{e}}\cdot\mathbf{r}|0\rangle|^2\gamma^2}{(\omega_{i0}-\omega)^2+\gamma^2} \quad (3)$$

where $|0\rangle$ denotes the ground state wave function; $|i\rangle$ is the wave function of the i^{th} excited state; and ω, $\hat{\mathbf{e}}$, $\mathbf{r}$, and α, respectively, represent the frequency of the incident light, polarization direction of the incident light, the position operator, and the fine structure constant. Furthermore, ω_{i0} is the energy difference (in frequency units) between the ground state ($|0\rangle$) and the i^{th} excited state ($|i\rangle$), while γ is the uniform lined width associated with each excited state energy level.

In eq 3, the summation over i indicates a sum over an infinite number of excited states, which we restrict for practical reasons to excited states with excitation energies up to 10 eV.

Time-Dependent Density Functional Theory Framework. We also performed first-principles time-dependent density functional theory (TDDFT) calculations to obtain the optical gap of these molecules, to validate our PPP-model based results. For this purpose, we employed a hybrid exchange-correlation functional B3LYP[35,36] and a localized Gaussian basis set, 6-31+G(d), as implemented in the GAUSSIAN16 package.[37] The B3LYP/6-31+G(d) combination can exhibit excellent comparison with the experiment, as demonstrated by Mocci et al.[38] recently for the parent molecule coronene and discussed by us later. Therefore, we have employed the identical methodology [B3LYP/6-31+G(d)] to study the electronic and optical properties of the PAHs considered in this work.

RESULTS AND DISCUSSION

In this section, we present and analyze the computed linear optical absorption spectra obtained using the CI approach and PPP model (PPP-CI approach, in short) for the five PAH molecules considered in this work. As mentioned earlier, for benzo[*ghi*]perylene, in addition to QCI calculations, MRSDCI calculations were also performed using the screened parameters in the PPP model, and the calculated absorption spectra are compared in Figure S1 of the Supporting Information. We note that the peak locations of the QCI spectra are somewhat blue-shifted as compared to the MRSDCI spectra, except for the first peak, whose position is almost the same in both the spectra. In spite of these small quantitative differences, the two spectra agree with each other quite well, qualitatively. This implies that the MRSDCI methodology is reliable, and therefore, calculations for the four larger coronene derivatives performed using that approach are trustworthy.

To emphasize the large-scale nature of our CI calculations, we present the total number of spin-adapted configurations (N_{total}), i.e., the dimension of the CI matrix in Table 1, for all the symmetries of each molecule. The large numbers of spin-adapted configurations considered in these calculations indicate that the electron-correlation effects have been included adequately. For the case of the smallest molecule benzo[*ghi*]-perylene, the total number of configurations employed in the MRSDCI calculations was close to one million, which is less

Table 1. N_{total} Represents the Total Number of Spin-Adapted Configurations Included in the CI Calculations for Each Symmetry of Coronene Derivatives Studied in This Work[a]

molecule	point group	symmetry	N^a_{total}	N^b_{total}
benzo[*ghi*]perylene	C_{2v}	A_1	2003907	2003907
($C_{22}H_{12}$)		B_2	3418335	3418335
benzo[*a*]coronene	C_{2v}	A_1	1107236	1359626
($C_{28}H_{14}$)		B_2	688351	1598428
naphtho[2,3*a*]coronene	C_{2v}	A_1	1252070	2611234
($C_{32}H_{16}$)		B_2	2018406	2622562
anthra[2,3*a*]coronene	C_{2v}	A_1	3541980	4778775
($C_{36}H_{18}$)		B_2	4034925	6002917
naphtho[8,1,2-*abc*] coronene	C_1	A	2054952	4200367
($C_{30}H_{14}$)				

[a]The superscripts "a" and "b" indicate the value of N_{total} employed in the PPP calculations based on the screened and the standard parameters, respectively. The QCI method was employed only for benzo[*ghi*]perylene, while for all other cases the MRSDCI approach was used.

https://dx.doi.org/10.1021/acs.jpcc.0c01719
J. Phys. Chem. C 2020, 124, 14297−14305

Table 2. Optical Gaps of Five PAH Molecules Calculated Using Tight-Binding (TB) and PPP Models, at Various Levels of Theory[a]

	H−L gap	H−L gap (in eV)		optical gap (in eV)		optical gap	optical gap
	(in eV)	PPP-RHF		PPP-CI		(in eV)	(in eV)
molecule	TB	scr	std	scr	std	TDDFT	experiment
benzo[*ghi*]perylene ($C_{22}H_{12}$)	2.11	3.85	7.13	3.39	3.54	3.19	-
benzo[*a*]coronene ($C_{28}H_{14}$)	2.25	3.95	7.13	3.42	3.44	3.13	3.38
naphtho[2,3*a*]coronene ($C_{32}H_{16}$)	1.89	3.57	6.71	2.93	3.32	2.83	-
anthra[2,3*a*]coronene ($C_{36}H_{18}$)	1.49	3.14	6.23	2.70	3.10	2.35	-
naphtho[8,1,2-*abc*]coronene ($C_{30}H_{14}$)	1.83	3.43	6.48	2.95	3.23	2.92	3.02

[a]For one-electron theories (TB, PPP-RHF), the HOMO−LUMO (H−L) gap is interpreted as the optical gap. For benzo[*ghi*]perylene, reported results are at the QCI level, while for the rest of the molecules they are at the MRSDCI level. In the last column, experimental values of the optical gaps (where available) are presented.

than half of those in the QCI calculations. In spite of that, good qualitative and quantitative agreement between the two sets of calculations implies that the MRSDCI approach is computationally efficient and accurate.

Optical Gap. In order to understand the influence of electron-correlation effects in a quantitative manner, in Table 2 we present the results on the HOMO−LUMO gap of these molecules using the independent-electron approaches, namely, the tight-binding (TB) model and the restricted Hartree−Fock (RHF) approach. Note that when we set $U = 0$ (i.e., no electron−electron interactions) in the PPP Hamiltonian (see eqs 1 and 2) we obtain the tight-binding model. The same table also contains the results on optical gaps of these molecules obtained using the PPP model and the CI approach. Optical gaps obtained from electron-correlated calculations are counterparts of the HOMO−LUMO gaps of one-electron theory.

From Table 2, it is obvious that: (a) for C_{2v} symmetry coronene derivatives the gaps decrease with the increasing size, independently of the models and the methods used in this work, (b) in the case of the TB model, the computed gaps are smaller than the results obtained using the PPP model; (c) the gaps obtained using the PPP-RHF level of theory with the standard parameters are much larger as compared to the other computed results; and (d) the optical gaps, calculated by employing the PPP-CI level of theory, are significantly red-shifted as compared to the gaps obtained from the PPP-RHF level of theory, especially with the standard parameter calculations. For screened parameter calculations, the correlation-induced shifts are small, and (e) the results of screened and standard parameters, obtained using the PPP-MRSDCI level of theory, are in good quantitative agreement with each for the smallest molecule but differ somewhat for the larger ones.

When we compare our optical gaps computed using the PPP-CI approach with those computed using the TDDFT method, we note that in all the cases TDDFT values are smaller than the PPP-CI values (see Table 2). Although for the case of naphtho[8,1,2-*abc*]coronene our PPP-CI band gaps computed using the screened parameters are only very slightly (0.03 eV) larger than the TDDFT value, for other molecules, the disagreement is quite significant. We hope that future measurements of band gaps of those molecules, for which no experimental data are available as of now, can resolve these differences. Regarding the comparison of the computation time for the PPP-CI and the TDDFT approaches, it depends on the level of CI approximation employed. It is well-known that the TDDFT approach is similar to CI-singles (CIS) in that both methods account for 1 particle−1 hole excitations. For the largest molecule, i.e., anthra[2,3*a*]coronene, the TDDFT approach took approximately 5 hours on our cluster, while CIS calculations finish in a matter of seconds. However, PPP-MRSDCI calculations for the same molecule took longer than a week because they employ a large number of configurations, some of which have 4 particle−4 hole character with respect to the Hartree−Fock meanfield.

Comparison with Coronene ($C_{24}H_{12}$). In a work involving our group, experimental measurements of the linear and nonlinear optical absorption of coronene molecule (D_{6h} symmetry) were performed, supported theoretically by calculations based on PPP-CI methodology. Measurements of linear absorption found the optical gap near 3.55 eV, characterized by very weak intensity, while the most intense peak was found to be at 4.1 eV.[11] Within the framework of first-principles time-dependent density functional theory (TDDFT), Mocci et al.[38] recently computed the location of the first and the most intense peak of this molecule to be 4.09 eV, in very good agreement with our calculated value of 4.20 eV,[11] thus validating our PPP-model-based methodology. Our PPP-model-based theory correctly predicted the most intense peak but was unable to predict the onset of weak absorption at 3.55 eV because the excited states near its location were found to be dipole forbidden due to electron−hole symmetry selection rules.[11] In the case of lower symmetry PAH molecules studied here, again, the optical gap is characterized by weak intensity. However, the corresponding optical transition is dipole allowed for these molecules, due to their lower symmetries. As far as quantitative comparison is concerned, for all the molecules studied here, the optical gap is lower than 3.55 eV measured for coronene.[11]

Linear Optical Absorption Spectrum. In this section, we present and discuss the calculated optical absorption spectra of the PAH molecules, considered in this work. The calculations were performed using the CI approach, and the spectra are plotted in Figures 3−6. Detailed information related to the excited states contributing to the spectra is presented in Tables S1−S10 of the Supporting Information.

A careful examination of the spectra illustrates the following important points: (a) spectra obtained from screened parameter are always red-shifted as compared to the absorption spectra computed using standard parameters, consistent with the similar shift observed for the HOMO−LUMO gap mentioned above; (b) with the increasing size, the absorption spectra are red-shifted for the C_{2v} symmetric coronene derivatives, and the first peak of the optical spectra appears due to the absorption of a

https://dx.doi.org/10.1021/acs.jpcc.0c01719
J. Phys. Chem. C 2020, 124, 14297−14305

photon, polarized along the *y*-direction because of a transition from their ground state ($^1A_1$) to the $^1B_2$ excited state characterized predominantly by the singly excited configuration $|H \rightarrow L\rangle$, corresponding to the optical gap. For the C_s symmetry structure, the first peak representing the optical gap is due to the absorption of a photon with mixed $x-y$ polarization, to a state dominated again by $|H \rightarrow L\rangle$ configuration. (c) The first peak obtained from the screened parameter calculations, is moderately intense, whereas the standard parameter calculations predict the first peak to be of relatively lower intensity for each molecule, and (d) the position of the first peak and higher energy peaks has a significant dependence on the Coulomb parameters employed in the calculations.

The experimental data for the optical gap are available only for benzo[*a*]coronene and naphtho[8,1,2-*abc*]coronene molecules, presented in the last column of the Table 2. It is obvious from the table that the PPP-CI approach predicts the optical gaps much more accurately as compared to the TB model and PPP-RHF approach. Therefore, we only compare the PPP-CI results with the experimental data, wherever available. The first peak (3.38 eV) of the experimentally obtained spectra of benzo[*a*]coronene is in good agreement with the screened parameter value (3.42 eV), as well as the standard parameter one (3.44 eV). For this case, TDDFT predicts a much lower value of 3.13 eV, which clearly underestimates the experimental band gap by about 0.25 eV. For naphtho[8,1,2-*abc*]coronene also, the experimental value of the optical gap (3.02 eV) is in good agreement with the screened parameter value (2.95 eV), but the standard parameter value (3.23 eV) is significantly higher. Here, the TDDFT-predicted value of 2.92 eV is in good agreement both with the experiment and our screened parameter based PPP-CI value. This suggests that our screened parameter PPP-CI values of the optical gaps of the two other molecules, for which no experimental results are available, are likely to be close to the true values. Next, we discuss our CI results for the higher energy regions of the absorption spectra of individual molecules.

Benzo[ghi]perylene ($C_{22}H_{12}$). The geometry of benzo[*ghi*]-perylene is presented in Figure 1(a), whereas its optical absorption spectra are depicted in Figure 2. We calculated the photoabsorption spectra by employing QCI methodology and the PPP model Hamiltonian employing both the screened and the standard Coulomb parameters. Detailed information related to the excited states contributing to the peaks of the optical absorption spectra is presented in Tables S1 and S2 of the Supporting Information.

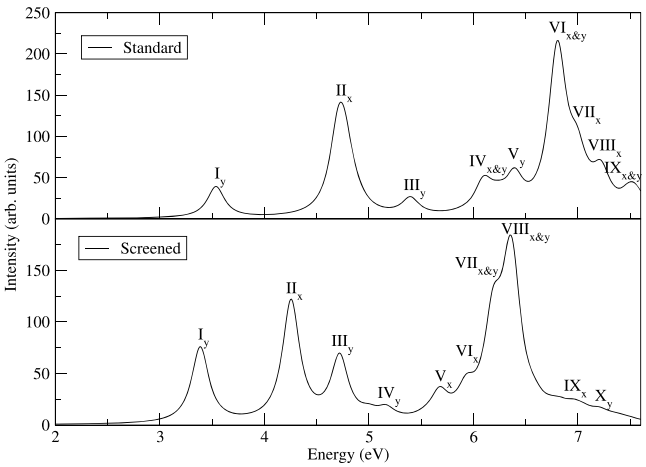

Figure 2. Linear optical absorption spectrum of benzo[*ghi*]perylene ($C_{22}H_{12}$) computed by employing the PPP-QCI methodology. Both the Coulomb parameters, screened, and standard, were separately used to compute the spectra. A uniform line width of 0.1 eV was adopted to plot the absorption spectra. Subscripts of peak labels indicate the polarization direction of the photon absorbed in the transition.

Figure 2 reveals that the spectra, computed using both the Coulomb parameters, have similar qualitative features. Because both the spectra begin with moderately intense peaks, the second peaks are intense peaks followed by several weaker peaks, and the most intense peaks appear at the higher energy region. Experimental data of the absorption spectra of this molecule are not available for comparison.

Now, we discuss the two intense peaks of the optical spectra obtained from both the Coulomb parameters. The second peak in both the spectra is due to the excited states, whose wave functions are dominated by the single excited configurations $|H - 1 \rightarrow L\rangle$ and $|H \rightarrow L + 1\rangle$. The most intense peak located at 6.35 eV (peak VIII, screened parameters) is due to two excited states whose wave functions are largely composed of $|H - 2 \rightarrow L + 4\rangle$, $|H - 4 \rightarrow L + 2\rangle$, $|H - 3 \rightarrow L + 4\rangle$, and $|H - 4 \rightarrow L + 3\rangle$. The most intense peak in the standard parameter spectrum near 6.8 eV (peak VI) is due to three excited states whose wave functions are composed mainly of the configurations $|H - 2 \rightarrow L + 3\rangle$, $|H - 3 \rightarrow L + 2\rangle$, $|H - 3 \rightarrow L + 3\rangle$, $|H - 2 \rightarrow L + 2\rangle$, $|H - 4 \rightarrow L + 2\rangle$, and $|H - 2 \rightarrow L + 4\rangle$.

Benzo[a]coronene ($C_{28}H_{14}$). The geometry of benzo[*a*]-coronene is presented in Figure 1(b). We computed the linear optical spectra of benzo[*a*]coronene, plotted in Figure 3, using

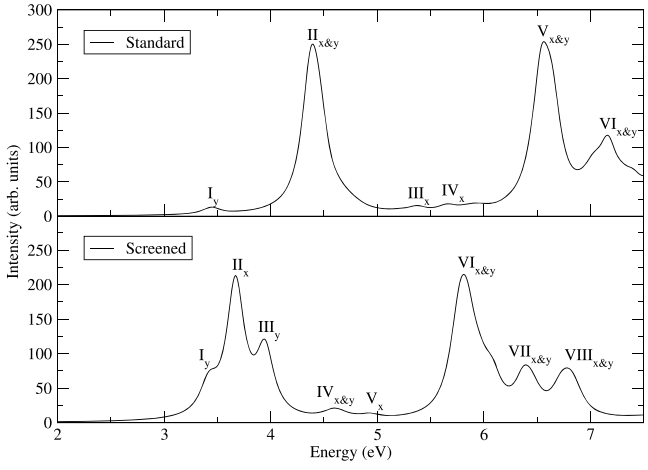

Figure 3. Linear optical absorption spectrum of benzo[*a*]coronene ($C_{28}H_{14}$) computed by employing our PPP-MRSDCI methodology. Both the Coulomb parameters, screened and standard, were separately used to compute the spectra. Uniform line width of 0.1 eV was adopted to plot the absorption spectra. Subscripts of peak labels indicate the polarization direction of the photon absorbed in the transition.

both the Coulomb parameters, screened and standard. The dominant configurations contributing to the wave functions of the excited states of the corresponding peaks are provided in Tables S3–S4 of the Supporting Information.

From Figure 3, it is obvious that, irrespective of the Coulomb parameters, there are two major peaks in the spectra, in addition to a number of less intense peaks. A solution-phase experimental study of optical absorption in this molecule was performed by Bagley et al.[25] Our screened parameter peak positions are compared to the measured ones in Table 3, and it is obvious that

https://dx.doi.org/10.1021/acs.jpcc.0c01719
J. Phys. Chem. C 2020, 124, 14297−14305

Table 3. Comparison of Experimental Peak Locations with Those Calculated Using the Screened Parameters, In the Absorption Spectrum of Benzo[*a*]coronene, Excluding the Optical Gap

molecule	symmetry	peak position (eV) exptl work[25]	peak position (eV) this work (theory)
benzo[a]coronene	-	3.47	-
($C_{28}H_{14}$)	$^1A_1$	3.61	3.67
	$^1B_2$	3.95	3.95
	-	4.09	-
	$^1B_2$	4.51	4.58
	$^1A_1$	4.65	4.66

the two sets of values are in generally very good agreement with each other. On the other hand, for these peaks, the agreement between the experimental values and the standard parameter results was poor. The optical absorption spectrum computed using the standard parameters exhibits only one intense peak, in addition to the first peak (peak I). While the location of peak I is in good agreement with the experimental data as discussed earlier, the disagreement in the location of this second peak is close to 22%. From Table 3, it is obvious that, except for two peaks located at 3.47 and 4.09 eV, the quantitative agreement between our screened parameter calculations and the experiments is excellent. Our screened parameter calculations also predict an intense peak (peak VI) near 5.80 eV; however, there is no experimental data available beyond 5.39 eV. We hope that in future experiments this higher energy region of the spectrum will be probed, to verify whether or not the predictions of our computed spectrum in that region hold.

Next, we analyze the wave functions of the excited states contributing to the two most intense peaks in the computed spectra. Peak II of both the spectra located at 3.67 eV (screened) and 4.38 eV (standard) is dominated by the singly excited configurations $|H \rightarrow L + 1\rangle$ and $|H - 1 \rightarrow L\rangle$, while the second intense features near 5.8 eV (peak VI, screened parameters) and 6.5 eV (peak V of standard parameters) are due to states whose wave functions are largely composed of the single excitations $|H - 3 \rightarrow L + 2\rangle$ and $|H - 2 \rightarrow L + 3\rangle$. For the weaker peaks of the absorption spectra, also the contributions to the wave functions of excited states are derived mainly from the singly excited configurations.

Naphtho[2,3a]coronene ($C_{32}H_{16}$). The geometry of the molecule is presented in Figure 1(c), whereas Figure 4 represents the linear optical photoabsorption spectra of naphtho[2,3*a*]coronene computed using the PPP-CI approach with screened and standard parameters, separately. The configurations with significant contribution to the peaks of the optical spectra are presented in Tables S5 and S6 of the Supporting Information with quantitative descriptions of some other parameters.

The spectra obtained using both sets of Coulomb parameters start with a very similar trend, and the second peaks of the absorption spectra, which are the most intense peaks, are followed by several weaker peaks. For this molecule, no experimental data are available for comparison with our computed photoabsorption spectra.

Next, we discuss the wave functions of the excited states contributing to intense peaks of the computed spectra. The most intense peaks (peak II) of both the spectra near 3.48 eV (screened) and 4.19 eV (standard) appear due to the states whose wave functions are characterized by the two equally

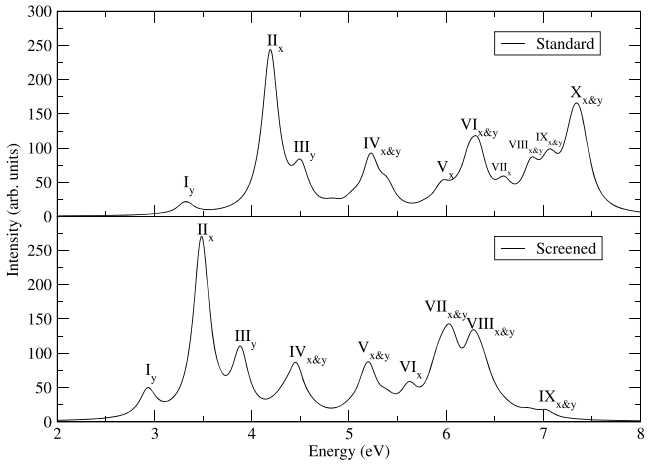

Figure 4. Linear optical absorption spectrum of naphtho[2,3*a*]-coronene ($C_{32}H_{16}$) computed by employing our PPP-MRSDCI methodology. Both the Coulomb parameters, screened and standard, were separately used to compute the spectra. Uniform line width of 0.1 eV was adopted to plot the absorption spectra. Subscripts of peak labels indicate the polarization direction of the photon absorbed in the transition.

contributing singly excited configurations $|H \rightarrow L + 1\rangle$ and $|H - 1 \rightarrow L\rangle$. Peak III near 3.88 eV (screened) and 4.50 eV (standard) is due to transitions to states whose wave functions are dominated by the single excitation $|H - 1 \rightarrow L + 1\rangle$ with the photon polarized along the *y*-direction. In the screened parameter spectrum, peaks VII (6.00 eV) and VIII (6.30 eV) are the last two closely spaced intense peaks. For peak VII, the excited state wave function is dominated by single excitation $|H - 3 \rightarrow L + 3\rangle$ and double excitations $|H - 2 \rightarrow L; H - 1 \rightarrow L\rangle$ and $|H \rightarrow L + 2; H \rightarrow L + 1\rangle$. The excited state corresponding to peak VIII, on the other hand, is strictly composed of the single excitations $|H - 4 \rightarrow L + 5\rangle$ and $|H - 5 \rightarrow L + 4\rangle$. The last peak (peak X, standard parameters) near 7.4 eV is due to a state whose wave functions are mainly derived from the singly excited configurations $|H - 3 \rightarrow L + 6\rangle$, $|H - 6 \rightarrow L + 3\rangle$, $|H - 9 \rightarrow L + 1\rangle$, and $|H - 1 \rightarrow L + 9\rangle$.

Anthra[2,3a]coronene ($C_{36}H_{18}$). Figure 5 presents the optical spectra of an anthra[2,3*a*]coronene molecule calculated using PPP-CI methodology with both screened and standard parameters. The dominant configurations contributing to the wave functions of the excited states of the corresponding peaks are provided in Tables S7 and S8 of the Supporting Information.

The spectra computed using the two sets of Coulomb parameters have similar qualitative features in that both start with a small peak, followed by the maximum intensity peak. The higher energy regions of the two spectra contain a series of low to moderate intensity peaks. For this molecule also no experimental data on its optical absorption are available.

The many-body wave functions of the excited states corresponding to the second peak of both the spectra, which are the most intense ones, are dominated by the equally contributing single excitations $|H \rightarrow L + 2\rangle$ and $|H - 2 \rightarrow L\rangle$, with the polarization along the *x*-direction. Peaks III of both the spectra appear near 4.1 eV (screened) and 4.7 eV (standard) due to the excited states whose many-body wave functions are composed of equally contributing singly excited configurations $|H \rightarrow L + 4\rangle$ and $|H - 4 \rightarrow L\rangle$. A moderately intense peak IX at 7.3 eV (standard) is dominated by the singly excited configurations $|H - 3 \rightarrow L + 3\rangle$ and $|H - 4 \rightarrow L + 4\rangle$, whereas

https://dx.doi.org/10.1021/acs.jpcc.0c01719
J. Phys. Chem. C 2020, 124, 14297−14305

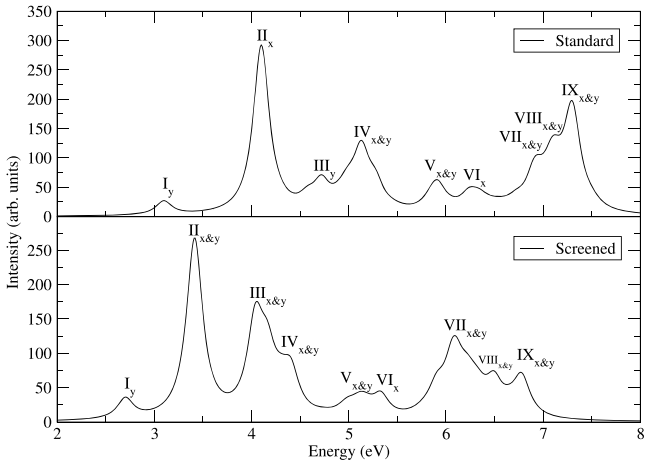

Figure 5. Linear optical absorption spectrum of anthra[2,3*a*]coronene ($C_{36}H_{18}$) computed by employing our PPP-MRSDCI methodology. Both the Coulomb parameters, screened and standard, were separately used to compute the spectra. Uniform line width of 0.1 eV was adopted to plot the absorption spectra. Subscripts of peak labels indicate the polarization direction of the photon absorbed in the transition.

peak VIII at 6.5 eV (screened) exhibits strong mixing of single and double excitations $|H - 6 \rightarrow L + 6\rangle$, $|H - 5 \rightarrow L + 5\rangle$, $|H \rightarrow L + 1; H \rightarrow L + 3\rangle$, and $|H - 1 \rightarrow L; H - 3 \rightarrow L\rangle$.

Naphtho[8,1,2-abc]coronene ($C_{30}H_{14}$). The linear optical spectra of naphtho[8,1,2-*abc*]coronene is presented in Figure 6

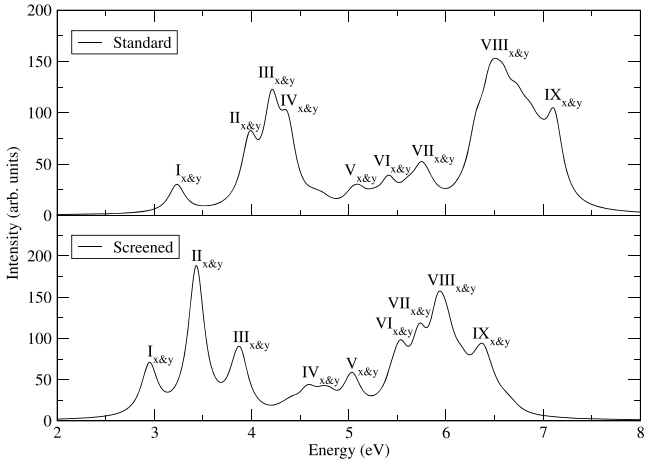

Figure 6. Linear optical absorption spectrum of naphtho[8,1,2-*abc*]coronene ($C_{30}H_{14}$) computed by employing our PPP-MRSDCI methodology. Both the Coulomb parameters, screened and standard, were separately used to compute the spectra. Uniform line width of 0.1 eV was adopted to plot the absorption spectra. Subscripts of peak labels indicate the polarization direction of the photon absorbed in the transition.

computed using both screened and standard parameters within the framework of PPP-CI methodology. The quantitative descriptions of the configurations of the wave functions contributing to the peaks of the optical spectrum are presented in Tables S9 and S10 of the Supporting Information. The results of calculations performed using the screened parameters are compared with the experimental data in Table 4.

From Figure 6, it is obvious that independent of Coulomb parameters employed both the spectra contain two intense peaks, in addition to a number of weaker peaks. Bagley and

Table 4. Comparison of Experimental Peak Locations with Those Calculated Using the Screened Parameters, In the Absorption Spectrum of Naphtho[8,1,2-*abc*]coronene, Excluding the Optical Gap

molecule	symmetry	peak position (eV) exptl work[25]	peak position (eV) this work (theory)
naphtho[8,1,2-*abc*]coronene	-	3.19	-
($C_{30}H_{14}$)	^1A	3.34	3.43
	-	3.62	-
	-	3.78	-
	^1A	3.95	3.89
	^1A	4.75−4.83	4.56−4.72

Wornat carried out an experimental study of optical absorption of this molecule in the solution phase.[25] In Table 4, we have compared only the screened parameter based results with the measured peaks[25] because we obtain much better agreement with those, as compared to standard parameter ones. For the second peak of the experimental spectrum at 3.19 eV, we find no candidate in our results. The location of the third experimental peak (3.34 eV) is in decent agreement with the second peak (3.43 eV) of our computed spectra. Then, two more experimental peaks (3.62 and 3.78 eV) are also absent in our calculations, but peak III of our calculations at 3.89 eV is near the experimentally obtained peak near 3.95 eV. The calculated set of peaks in the range 4.56−4.72 eV slightly underestimates the experimental peaks in the 4.75−4.83 eV energy range.[25] Our calculated spectrum contains several peaks in the higher energy region as well. However, the experimental data terminate at 4.9 eV.[25] Therefore, we hope that future experiments will extend to energies higher than this.

Now we discuss the wave functions of the excited states contributing to the peaks of the absorption spectra. The most intense peaks near 3.4 eV (screened) and 4.2 eV (standard) of both the absorption spectra are dominated by the singly excited configurations $|H - 1 \rightarrow L\rangle$ and $|H \rightarrow L + 1\rangle$, but the intense peaks obtained from the standard parameters are comparatively broader. The second intense peaks of both the optical spectra near 5.9 eV (screened) and 6.6 eV (standard) are broader and appear due to the states whose wave functions consist mainly of single excitations $|H - 3 \rightarrow L + 4\rangle$, $|H - 4 \rightarrow L + 3\rangle$ and $|H - 2 \rightarrow L + 6\rangle$, $|H - 6 \rightarrow L + 2\rangle$, respectively.

CONCLUSIONS

We calculated the optical properties of five different PAH molecules, namely, benzo[*ghi*]perylene ($C_{22}H_{12}$), benzo[*a*]-coronene ($C_{28}H_{14}$), naphtho[2,3*a*]coronene ($C_{32}H_{16}$), anthra-[2,3*a*]coronene ($C_{36}H_{18}$), and naphtho[8,1,2-*abc*]coronene ($C_{30}H_{14}$), by employing the large-scale electron-correlated PPP-CI methodology. For the sake of comparison, we also computed the optical gaps of these molecules using first-principles TDDFT. The common structural feature of these molecules is their similarity to coronene. Our computed spectra of benzo[*a*]coronene and naphtho[8,1,2-*abc*]coronene obtained by the PPP-CI approach are in good agreement with available experimental data. We hope for future experimental efforts to measure the higher energy region of optical spectra of these two molecules and photoabsorption spectra of the other three molecules, i.e., benzo[*ghi*]perylene, naphtho[2,3*a*]-coronene, and anthra[2,3*a*]coronene, against which our results

https://dx.doi.org/10.1021/acs.jpcc.0c01719
J. Phys. Chem. C 2020, 124, 14297−14305

could be benchmarked. A few important conclusions, which can be drawn from our calculations, are:

1. Our screened parameter PPP-CI results predict moderately intense absorption at the optical gap, while the standard parameter predicts a much smaller intensity.
2. For C_{2v} symmetry coronene derivatives, the computed optical spectra are red-shifted with the increasing size of the molecules, and the distance between the first two peak locations is also gradually increasing.
3. The computed optical spectra obtained using the screened parameters are in better agreement with the experimental data as compared to the standard parameter results.
4. The fact that we obtain good agreement of our PPP-CI calculations with the available experimental data implies that the $\sigma-\pi$ separation hypothesis which forms the basis of the PPP model is physically correct when it comes to the description of optical transitions in these molecules.
5. As compared to the coronene molecule, the optical gaps of all the four coronene derivatives studied here are smaller.
6. Optical gaps computed by the TDDFT approach were found to be lower than the corresponding PPP-CI values, for all the molecules.

As far as future directions are concerned, it will be interesting to probe photoinduced excited state absorptions from the optical gap of these molecules. Given the fact that none of these molecules have inversion symmetry, it will be interesting to investigate whether or not they exhibit second-order optical nonlinearities. Additionally, electroabsorption spectra of these molecules may provide further useful information about the nature of their low-lying excited states. Triplet excited states of these molecules may shed some light on the influence of electron correlation effects. At present, calculations along these directions are underway in our group, and the results will be reported in future works.

■ ASSOCIATED CONTENT

Supporting Information

The Supporting Information is available free of charge at https://pubs.acs.org/doi/10.1021/acs.jpcc.0c01719.

Comparison of the optical absorption spectra of the benzo[*ghi*]perylene molecule computed using the QCI and MRSDCI methods, employing the screened parameters in the PPP model. This is followed by a series of tables containing information about the excited states contributing to important peaks in the calculated absorption spectra of the lower-symmetry polycyclic aromatic hydrocarbon molecules considered in this work (PDF)

■ AUTHOR INFORMATION

Corresponding Authors

Pritam Bhattacharyya − *Department of Physics, Indian Institute of Technology Bombay, Powai, Mumbai 400076, India*; Email: pritambhattacharyya01@gmail.com

Deepak Kumar Rai − *Department of Physics, Indian Institute of Technology Bombay, Powai, Mumbai 400076, India*; Email: deepakrai@phy.iitb.ac.in

Alok Shukla − *Department of Physics, Indian Institute of Technology Bombay, Powai, Mumbai 400076, India*; orcid.org/0000-0002-0839-2956; Email: shukla@phy.iitb.ac.in

Complete contact information is available at: https://pubs.acs.org/10.1021/acs.jpcc.0c01719

Notes

The authors declare no competing financial interest.

■ ACKNOWLEDGMENTS

The work of P.B. was supported by a Senior Research Fellowship offered by University Grants Commission, India.

■ REFERENCES

(1) Sekitani, T.; Someya, T. Stretchable, Large-area Organic Electronics. *Adv. Mater.*. *22*, 2228−2246.

(2) Ma, H.; Yip, H.-L.; Huang, F.; Jen, A. K.-Y. Interface Engineering for Organic Electronics. *Advanced Functional Materials*. *20*1371−1388.

(3) Lüssem, B.; Keum, C.-M.; Kasemann, D.; Naab, B.; Bao, Z.; Leo, K. Doped Organic Transistors. *Chem. Rev.* **2016**, *116*, 13714−13751.

(4) Lei, T.; Pochorovski, I.; Bao, Z. Separation of Semiconducting Carbon Nanotubes for Flexible and Stretchable Electronics Using Polymer Removable Method. *Acc. Chem. Res.* **2017**, *50*, 1096−1104.

(5) Facchetti, A. pi-Conjugated Polymers for Organic Electronics and Photovoltaic Cell Applications. *Chem. Mater.* **2011**, *23*, 733−758.

(6) Luo, H.; Liu, Z.; Zhang, D. Conjugated D-A terpolymers for organic field-effect transistors and solar cells. *Polym. J.* **2018**, *50*, 21−31.

(7) Liu, Y.; Li, C.; Ren, Z.; Yan, S.; Bryce, M. R. All-organic thermally activated delayed fluorescence materials for organic light-emitting diodes. *Nature Reviews Materials* **2018**, *3*, 18020.

(8) Burroughes, J. H.; Bradley, D. D. C.; Brown, A. R.; Marks, R. N.; Mackay, K.; Friend, R. H.; Burns, P. L.; Holmes, A. B. Light-emitting diodes based on conjugated polymers. *Nature* **1990**, *347*, 539.

(9) Friend, R. H.; Gymer, R. W.; Holmes, A. B.; Burroughes, J. H.; Marks, R. N.; Taliani, C.; Bradley, D. D. C.; Santos, D. A. D.; Brédas, J. L.; Lögdlund, M.; et al. Electroluminescence in conjugated polymers. *Nature* **1999**, *397*, 121.

(10) Guo, F.; Karl, A.; Xue, Q.-F.; Tam, K. C.; Forberich, K.; Brabec, C. J. The fabrication of color-tunable organic light-emitting diode displays via solution processing. *Light: Sci. Appl.* **2017**, *6*, e17094.

(11) Aryanpour, K.; Roberts, A.; Sandhu, A.; Rathore, R.; Shukla, A.; Mazumdar, S. Subgap Two-Photon States in Polycyclic Aromatic Hydrocarbons: Evidence for Strong Electron Correlations. *J. Phys. Chem. C* **2014**, *118*, 3331−3339.

(12) Pople, J. A. Electron interaction in unsaturated hydrocarbons. *Trans. Faraday Soc.* **1953**, *49*, 1375−1385.

(13) Pariser, R.; Parr, R. G. A Semi-Empirical Theory of the Electronic Spectra and Electronic Structure of Complex Unsaturated Molecules. II. *J. Chem. Phys.* **1953**, *21*, 767−776.

(14) Aryanpour, K.; Shukla, A.; Mazumdar, S. Electron correlations and two-photon states in polycyclic aromatic hydrocarbon molecules: A peculiar role of geometry. *J. Chem. Phys.* **2014**, *140*, 104301.

(15) Shukla, A. Correlated theory of triplet photoinduced absorption in phenylene-vinylene chains. *Phys. Rev. B: Condens. Matter Mater. Phys.* **2002**, *65*, 125204.

(16) Shukla, A. Theory of nonlinear optical properties of phenyl-substituted polyacetylenes. *Phys. Rev. B: Condens. Matter Mater. Phys.* **2004**, *69*, 165218.

(17) Chakraborty, H.; Shukla, A. Pariser-Parr-Pople Model Based Investigation of Ground and Low-Lying Excited States of Long Acenes. *J. Phys. Chem. A* **2013**, *117*, 14220−14229.

(18) Chakraborty, H.; Shukla, A. Theory of triplet optical absorption in oligoacenes: From naphthalene to heptacene. *J. Chem. Phys.* **2014**, *141*, 164301.

(19) Sony, P.; Shukla, A. Large-scale correlated calculations of linear optical absorption and low-lying excited states of polyacenes: Pariser-Parr-Pople Hamiltonian. *Phys. Rev. B: Condens. Matter Mater. Phys.* **2007**, *75*, 155208.

(20) Rai, D. K.; Chakraborty, H.; Shukla, A. Tunable Optoelectronic Properties of Triply Bonded Carbon Molecules with Linear and Graphyne Substructures. *J. Phys. Chem. C* **2018**, *122*, 1309−1317.
(21) Basak, T.; Chakraborty, H.; Shukla, A. Theory of linear optical absorption in diamond-shaped graphene quantum dots. *Phys. Rev. B: Condens. Matter Mater. Phys.* **2015**, *92*, 205404.
(22) Basak, T.; Shukla, A. Optical signatures of electric-field-driven magnetic phase transitions in graphene quantum dots. *Phys. Rev. B: Condens. Matter Mater. Phys.* **2016**, *93*, 235432.
(23) Basak, T.; Basak, T.; Shukla, A. Electron correlation effects and two-photon absorption in diamond-shaped graphene quantum dots. *Phys. Rev. B: Condens. Matter Mater. Phys.* **2018**, *98*, 035401.
(24) Khan, Z. H. Electronic spectra of radical cations and their correlation with photoelectron spectra-III. Perylenes and coronenes. *Spectrochimica Acta Part A: Molecular Spectroscopy* **1988**, *44*, 313−320.
(25) Bagley, S. P.; Wornat, M. J. Identification of Six- to Nine-Ring Polycyclic Aromatic Hydrocarbons from the Supercritical Pyrolysis of n-Decane. *Energy Fuels* **2013**, *27*, 1321−1330.
(26) Fetzer, J. C. THE CHEMISTRY AND ANALYSIS OF LARGE PAHs. *Polycyclic Aromat. Compd.* **2007**, *27*, 143−162.
(27) Acree, W. E.; Tucker, S. A.; Zvaigzne, A. I.; Street, K. W.; Fetzer, J. C.; Grutzmacher, H.-F. Polycyclic Aromatic Hydrocarbon Solute Probes. Part VII: Evaluation of Additional Coronene Derivatives as Possible Solvent Polarity Probe Molecules. *Appl. Spectrosc.* **1990**, *44*, 477−482.
(28) Ohno, K. Some remarks on the Pariser-Parr-Pople method. *Theoretica chimica acta* **1964**, *2*, 219−227.
(29) Chandross, M.; Mazumdar, S. Coulomb interactions and linear, nonlinear, and triplet absorption in poly(para-phenylenevinylene). *Phys. Rev. B: Condens. Matter Mater. Phys.* **1997**, *55*, 1497−1504.
(30) McMurchie, L. E.; Elbert, S. T.; Langhoff, S. R.; Davidson, E. R. *MELD package from Indiana University*; 1993. It has been modified by us to handle bigger systems.
(31) Sony, P.; Shukla, A. A general purpose Fortran 90 electronic structure program for conjugated systems using Pariser-Parr-Pople model. *Comput. Phys. Commun.* **2010**, *181*, 821−830.
(32) Bhattacharyya, P.; Rai, D. K.; Shukla, A. Systematic First-Principles Configuration-Interaction Calculations of Linear Optical Absorption Spectra in Silicon Hydrides: Si2H2n (n = 1−3). *J. Phys. Chem. A* **2019**, *123*, 8619−8631.
(33) Bhattacharyya, P.; Boustani, I.; Shukla, A. First principles study of structural and optical properties of B12 isomers. *J. Phys. Chem. Solids* **2019**, *133*, 108−116.
(34) Shinde, R.; Shukla, A. Large-scale first principles configuration interaction calculations of optical absorption in aluminum clusters. *Phys. Chem. Chem. Phys.* **2014**, *16*, 20714−20723.
(35) Becke, A. D. Density-functional thermochemistry. III. The role of exact exchange. *J. Chem. Phys.* **1993**, *98*, 5648−5652.
(36) Lee, C.; Yang, W.; Parr, R. G. Development of the Colle-Salvetti correlation-energy formula into a functional of the electron density. *Phys. Rev. B: Condens. Matter Mater. Phys.* **1988**, *37*, 785−789.
(37) Frisch, M. J.; Trucks, G. W.; Schlegel, H. B.; Scuseria, G. E.; Robb, M. A.; Cheeseman, J. R.; Scalmani, G.; Barone, V.; Petersson, G. A.; Nakatsuji, H. et al. *Gaussian 16*, revision C.01; Gaussian Inc.: Wallingford CT, 2016.
(38) Mocci, P.; Cardia, R.; Cappellini, G. A computational study on the electronic and optical properties of boron-nitride circumacenes. *Phys. Chem. Chem. Phys.* **2019**, *21*, 16302−16309.

https://dx.doi.org/10.1021/acs.jpcc.0c01719
J. Phys. Chem. C 2020, 124, 14297−14305